In-situ Infrared Characterization During Atomic Layer Deposition of Lanthanum Oxide

In Situ Infrared Characterization during Atomic Layer Deposition of Lanthanum Oxide

Jinhee Kwon,*,† Min Dai,‡ Mathew D. Halls,§ Erik Langereis,|| Yves J. Chabal,† and Roy G. Gordon⊥

Department of Materials Science and Engineering, University of Texas at Dallas, Richardson, Texas 75080, Laboratory for Surface Modification, Rutgers University, Piscataway, New Jersey 08854, Materials Science Division, Accelrys Inc., San Diego, California 92121, Applied Physics, Plasma and Materials Processing, Eindhoven University of Technology, Eindhoven, The Netherlands, Department of Chemistry and Chemical Biology, Harvard University, Cambridge, Massachusetts 02138

Received: July 8, 2008; Revised Manuscript Received: November 5, 2008

Mechanisms of atomic layer deposition (ALD) growth of lanthanum oxide on H-terminated Si(111) using lanthanum tris(*N*,*N*′-diisopropylacetamidinate) (La(*i*Pr-MeAMD)$_3$) are investigated using infrared (IR) absorption spectroscopy. The reactivity of this amidinate precursor is high, with almost all surface Si−H bonds consumed after 5 ALD cycles at 300 °C. Gas phase IR spectra show that, although most of the precursor (La(*i*Pr-MeAMD)$_3$) remains intact, a strong feature at 1665 cm^{-1}, characteristic of a hydrogenated and dissociated free ligand with localized electrons in the N−C═N bonds, is present. Such partial precursor dissociation in the gas phase is due to hydrolysis by traces of water vapor remaining in the reactor, even after purging. As a result, some Si−O−La bonds are formed upon reaction with the surface during the first La(*i*Pr-MeAMD)$_3$ pulse, prior to any water pulse. During film growth, acetate/carbonate and hydroxyl impurities are incorporated into the film. Annealing to 500 °C in dry N_2 removes these impurities but fosters the growth of interfacial SiO_2. Deposition at 300 °C leads to decomposition of adsorbed ligands, as evidenced by the formation of cyanamide or carbodiimide vibrational bands (or both) at 1990 and 2110 cm^{-1}, respectively. Despite this decomposition, ideal self-limited ALD growth is maintained because the decomposed ligands are removed by the subsequent water pulse. Growth of pure lanthanum oxide films is often characterized by nonuniform film thickness if purging is not complete because of reversible absorption of water by the La_2O_3 film. Uniform ALD growth can be maintained without a rigorous dry purge by introducing alternating trimethylaluminum (TMA)/D_2O ALD cycles between La/D_2O cycles.

I. Introduction

Atomic layer deposition (ALD) of a variety of thin film materials is being thoroughly investigated because of the thickness and composition control and uniformity that it provides, even on structured substrates.[1] ALD is a modified chemical vapor deposition (CVD) process in which each precursor is introduced into a reactor alternatively separated by a purging/pumping process. When compared to CVD, the self-saturation for each precursor leads to a good interface quality and better step coverage of high-aspect ratio features. ALD is also a lower temperature process than CVD. The precursor chemistry at the surface is critical for successful ALD growth. Indeed, the small number of suitable ALD precursors limits wider applications of the technique. To make ALD growth possible, precursors must satisfy many stringent criteria, such as thermal stability, high volatility, and efficient self-limited reactivity with surfaces. The reactions on the surface and during growth must be as complete as possible to minimize incorporation of impurities in the films.

Recently, amidinate ($[R^1NC(R^2)NR^3]^-$) ligands have been incorporated into transition metal and lanthanide catalysts.[2−5] These catalysts are used in solution, so the volatility of these amidinate compounds was never tested. In fact, these catalytic amidinate compounds have usually been made with large, heavy substituents that preclude any volatility. In addition, many catalysts are used as ionic complexes that are not volatile. Thus amidinate compounds had not been considered as possible precursors for ALD until recently, when a number of volatile metal amidinates were synthesized[6] and their suitability for ALD was demonstrated.[7] Metal amidinates have a number of advantages as ALD precursors. Because they have no M−C bonds, carbon incorporation into the films may be suppressed, and the relatively reactive M−N bonds make low-temperature deposition possible. Their steric and electronic properties can be easily tailored through variations of C- and N-substituents.[8] Amidinate ligands are also known to enhance the thermodynamic stability of their complexes due to the chelating effect of the bidentate ligands.[9,10] Some transition metals, such as Cu, Co, Fe, Ru, Mn, and Ni, as well as their nitrides and oxides and rare earth oxides have been successfully grown by ALD from the corresponding amidinate precursors.[7,11−16] However, the surface chemistry of these relatively new precursors has not yet been investigated in situ, because most studies to-date have focused on ex situ film characterization by electrical, physical, or chemical measurements.

The present work focuses on initial surface nucleation mechanisms, amidinate ligand elimination, precursor decomposition and contamination incorporation, and interface evolution during ALD using in situ Fourier transform infrared spectroscopy (FTIR). For this study, we use lanthanum tris(*N*,*N*′-diisopropylacetamidinate) (La(*i*Pr-MeAMD)$_3$) and water (D_2O)

* Corresponding author. E-mail: jinhee@utdallas.edu.
† University of Texas at Dallas.
‡ Rutgers University.
§ Accelrys Inc.
|| Eindhoven University of Technology.
⊥ Harvard University.

10.1021/jp806027m CCC: $40.75
Published on Web 12/19/2008

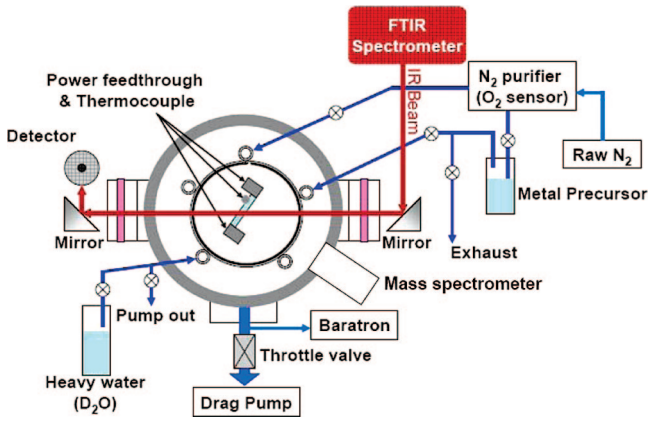

Figure 1. Schematic diagram of the ALD reactor connected to an IR spectrometer for in situ surface characterization. KBr windows for IR transmission are protected by gate valves to isolate them during ALD precursor exposures.

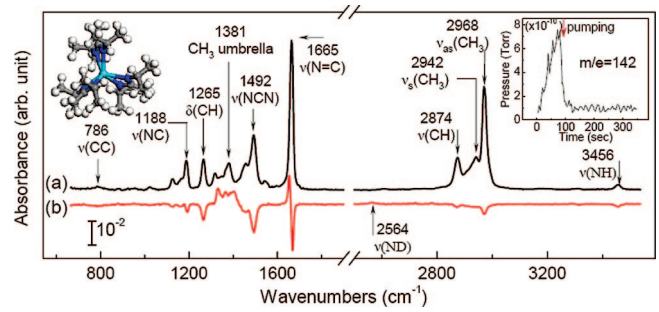

Figure 2. (a) FTIR absorption spectrum of gas phase La(^{i}Pr-MeAMD)$_3$ (source temperature 125 °C) at 0.13 Torr, measured after it is introduced into the evacuated (0.08 Torr) reactor (used as reference). (b) Differential spectrum of the La(^{i}Pr-MeAMD)$_3$ precursor after D_2O is introduced, using the original La(^{i}Pr-MeAMD)$_3$ spectrum (a) as reference. The inset in the left shows the ball-and-stick structure of the intact precursor, where the light blue, blue, gray, and white balls represent La, N, C, and H atoms, respectively. The inset in the right shows QMS measurement during La(^{i}Pr-MeAMD)$_3$ pulse monitoring $m/e = 142$.

for ALD growth of lanthanum oxide, one of the potential candidates for a high-permittivity ($\kappa = \sim 20-27$) gate dielectric for future complementary metal oxide semiconductor (CMOS) devices.[17−20] The synthesis and properties of La(^{i}Pr-MeAMD)$_3$ have been described by Gordon et al.[6] This precursor molecule has higher volatility (80 °C/0.04 Torr)[6] than previously known lanthanum sources and has been successfully demonstrated for the growth of both lanthanum oxide and lanthanum aluminate.[21] A similar precursor, lanthanum tris(*N*,*N*′-diisopropylformamidinate) is slightly more volatile and is expected to have surface chemistry similar to that of the precursor that we studied.[22]

II. Experimental Section

For this study, double-sided polished, float-zone-grown (lightly B-doped, $\rho \sim 10\ \Omega$ cm) Si(111) wafers are used. Atomically flat hydrogen-terminated Si(111) surfaces are prepared by immersion for 1 min in HF (~20%) and for 2 min in NH_4F (~49%) after RCA[23] cleaning. The lanthanum precursor (La(^{i}Pr-MeAMD)$_3$) is kept at ~130 °C, and the Si sample temperature is varied between 200 and 300 °C. Heavy water (D_2O) is used instead of H_2O to distinguish infrared vibrational bands related to growth chemistry from environmental water. H-terminated Si samples are immediately loaded in a nitrogen (oxygen impurity $<10^{-5}$ ppm)-purged reactor. Growth is performed in a home-built ALD reactor connected to a FTIR spectrometer (Thermo Nicolet 6700, frequency range of 400−4000 cm^{-1}); its schematic is shown in Figure 1. A single-transmission geometry (74° incidence) is used to optimize the study of modes in the 500−1500 cm^{-1} regions, minimize interferences and give good sensitivity to modes polarized perpendicular to the interface.[24] The transmitted IR beam is focused onto a broadband mercury cadmium telluride (MCT/B) detector. The KBr windows for IR transmission are isolated during ALD precursor exposures by closing two gate valves located in front of the windows. Lanthanum tris(*N*,*N*′-diisopropylacetamidinate) carried by ultrapure N_2 gas and water (D_2O) are delivered alternatively to the ALD reactor through stainless steel tubing. After each precursor pulse, the reactor is purged and pumped for at least 5 min with ultrapure N_2 gas to prevent cross gas phase reactions among precursors (i.e., CVD) and to eliminate byproducts after surface reactions. The reactor is also equipped with a differentially pumped quadrupole mass spectrometer (QMS, Stanford Research Systems) for gas phase analysis. Rutherford backscattering spectroscopy (RBS) characterization of lanthanum oxide films is performed ex situ with 2 MeV He^+ ions. The detector is placed at a 160° backscattering angle with respect to the surface normal to measure La density.

First-principles calculations based on density functional theory (DFT) are carried out to aid in the interpretation of infrared (IR) features of the intact La precursor with three amidinate ligands (LaL_3) and of an isolated amidine (a hydrogenated ligand, HL), where L represents a ligand. Gradient-corrected PBE functionals[25] are used, as implemented in the DMol3 package.[26] A numerical atomic basis set of double-ζ quality, augmented with additional polarization functions (DNP) with a real-space cutoff of 5.8 Å is employed in this work. For La, the core electrons are represented with an effective relativistic semicore pseudopotential along with the DNP basis for valence electrons.[27] The convergence criteria for structural optimizations are 1.0×10^{-7} au and 1.0×10^{-5} au/Å for energy and gradient, respectively.

III. Results and Discussion

Gas phase species in the ALD reactor are first investigated to determine the state of the precursor prior to reaching the sample. Figure 2a shows FTIR spectrum of the gas phase amidinate lanthanum precursor La(^{i}Pr-MeAMD)$_3$ after it is introduced into the reactor (0.13 Torr). All the modes associated with an intact precursor are observed; notably, the terminal methyl groups (CH_3) at 2968 cm^{-1} (asymmetric stretching), 2942 cm^{-1} (symmetric stretching), 1381 cm^{-1} (umbrella deformation), and CH at 1317 cm^{-1} and 1265 cm^{-1} (bending) and weaker C−C modes at 786 cm^{-1}. When the precursor is intact with three chelating ligands, the π-electrons within the double bonds of the N−C−N linkage are delocalized, leading to a mode at 1492 cm^{-1}. Although this delocalized N−C−N mode has been placed at 1665 cm^{-1} by Wilkins in 1974,[28] we show below that the strong mode at 1665 cm^{-1} and weaker mode at 3456 cm^{-1} are actually due to free amidine (HL) arising from the reaction of the precursor LaL_3 with trace water.

Precursor dissociation in the presence of water would lead to the formation of a dissociated ligand with H attached (HL), producing two distinct species: (i) HN(^{i}Pr) −C(Me)=N(^{i}Pr) with distinct single and double bonds and (ii) LaL_2OH. To assist in assigning the observed bands and establish support for the appearance of the free ligand, DFT calculations at the PBE/DNP level of theory are carried out to obtain vibrational frequencies, intensities, and normal modes for the parent

TABLE 1: Calculated PBE/DNP Wavenumbers and General Mode Assignments Corresponding to the Key Observed Infrared Bands (indicated in Figure 2) Based on Calculations for the intact La Precursor (LaL_3), the Hydrolysis Product LaL_2OH, and Free Ligand HL

observed IR (cm^{-1})	calcd[a] (cm^{-1})	species	assignment
3456/2564	3464/2534	HL/DL	NH(ND) stretching
2968	3110 (3033) (3020)	HL (LaL_3) [LaL_2OH]	CH_3 asym stretching
2942	2950 (2948)	LaL_3 [LaL_2OH]	CH_3 sym stretching
2874	2970 (2876) (2891)	HL (LaL_3) [LaL_2OH]	CH stretching
1665/1659	1636/1625	HL/DL	C═N stretching
1492	1517 (1506)	LaL_3 [LaL_2OH]	NCN stretching + CH_3 scissor deformation
1450	1463 (1456)	LaL_3 [LaL_2OH]	NCN stretching + CH_3 scissor deformation
1381	1377 (1377) (1374)	HL (LaL_3) [LaL_2OH]	CH_3 umbrella + CH bending
1317	1355 (1333)	LaL_3 [LaL_2OH]	CH wagging
1265	1304 (1303)	LaL_3 [LaL_2OH]	CH bending
1188	1185 (1193) (1193)	HL (LaL_3) [LaL_2OH]	CN stretching + CH_3 rocking
1126	1159 (1158)	LaL_3 [LaL_2OH]	CH_3 rocking + NCN stretching
1022	1052 (1052)	LaL_3 [LaL_2OH]	CH_3 rocking + NCN bending
786	774 (774)	LaL_3 [LaL_2OH]	CC stretching

[a] PBE/DNP calculated harmonic frequencies.

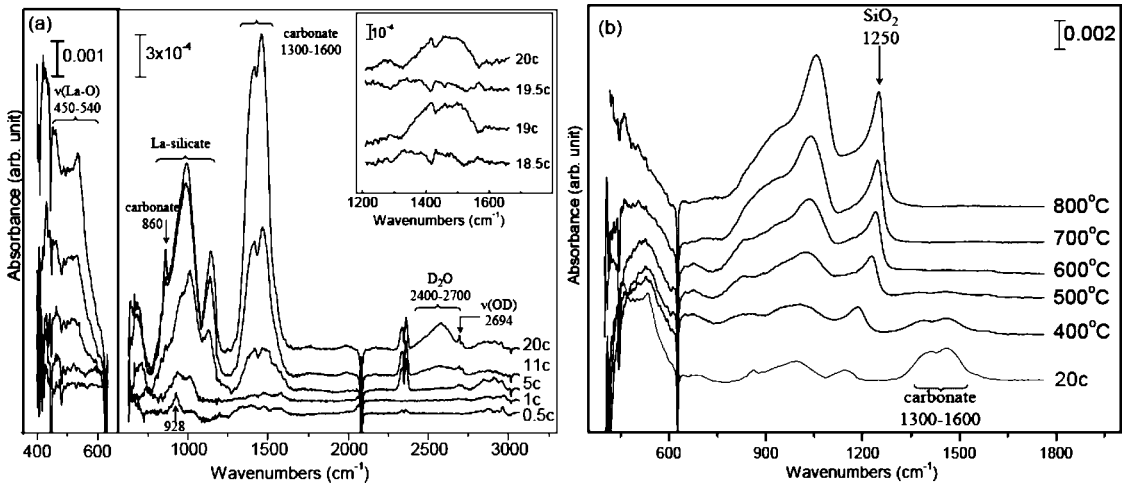

Figure 3. (a) FTIR absorption spectra of H/Si(111) after subsequent exposures to La(^{i}Pr-MeAMD)$_3$ (0.5c), D_2O (1c) and 5th, 11th, and 20th ALD cycles with the Si sample at 200 °C. The inset shows the differential spectra of half-cycles from the 18.5th to 20th cycles in the carbonate/acetate absorption range. (b) FTIR absorption spectra measured after postdeposition annealing from 400 to 800 °C with 100 °C increments in dry N_2 (0.68 Torr). All spectra are referenced to the initial H-terminated Si(111) surface.

precursor LaL_3, the hydrolysis product LaL_2OH, and the free ligand HL, for comparison with experiment. Calculations for the free ligand show that the band at 1665 cm^{-1} (calcd 1636 cm^{-1}) should be assigned to the localized *C*═N stretching of HN−C═N bonds in the hydrolyzed ligand (HL) rather than to the intact precursor LaL_3. La(^{i}Pr-MeAMD)$_3$ is known to be very reactive with water. Thus, HL may have been produced out of the reaction with trace water molecules in the reactor. Real-time mass spectroscopy (see the inset of Figure 2) in the ALD reactor confirms that a gas phase molecule with atomic mass 142 is produced, which corresponds to the HL species. Since HL is nonreactive, it remains in the gas phase and is preferentially detected by mass spectroscopy. It also does not affect film growth during the ALD process. In contrast, the LaL_2OH product is not readily detected by mass spectrometry because it adsorbed/reacts on the reactor surfaces.

Figure 2b shows the spectral changes (differential spectra) occurring after exposing the lanthanum precursor to water (D_2O). Most of the methyl-related bands of the La(^{i}Pr-MeAMD)$_3$ precursor lose intensity, and some new bands are observed between 1300 and 1430 cm^{-1} after D_2O exposure. The N−H stretching at 3456 cm^{-1} is shifted to 2564 cm^{-1} due to isotope replacement (N−D), calculated in DFT at 3464 and 2534 cm^{-1}. The isotope effect is also evident for the *C*═N stretching of N−C═N in the HL (DL) free ligand that shifts from 1665 to 1659 cm^{-1}. Calculations show a corresponding red shift of ~11 cm^{-1} with the H/D exchange. Table 1 presents a comparison of observed and computed IR wavenumbers and band assignments for the key modes discussed here and those of substantial intensity indicated in Figure 2.

The initial interaction of the precursor with the H-terminated Si(111) surface and subsequent ALD growth are investigated next. Figure 3a shows the FTIR absorption spectra of H/Si(111) exposed to the first La(^{i}Pr-MeAMD)$_3$ (0.5c), D_2O (1c) and 5th, 11th, and 20th cycles of ALD with the substrate at 200 °C. The decrease in the Si−H stretch intensity at 2083 cm^{-1} indicates that the La(^{i}Pr-MeAMD)$_3$ precursor readily reacts with the atomically flat H/Si(111) surface. The first La(^{i}Pr-MeAMD)$_3$ pulse consumes about 40% of the surface hydrogen and more than 80% of the surface H by the end of the fifth cycle. Rutherford backscattering (RBS) measurements show ~3 × 10^{14} cm^{-2} La atoms are on the surface after the first ALD cycle, corresponding to ~40% of the 7.8 × 10^{14} cm^{-2} H density on Si(111). This indicates that for each reacted hydrogen, there is one La atom, confirming the following reaction: LaL_3 + SiH → Si−LaL_2 + HL(g). As we show below, the bonding to Si is actually mediated by an oxygen atom, forming Si−O−LaL_2.

The absorption spectrum measured after the first La precursor exposure (0.5c) in Figure 3a shows a feature at 928 cm^{-1} assigned to the Si−O−La stretching mode.[29] Partial hydrolysis of the precursor into LaL_2OH due to traces of water vapor in the reactor makes it possible to form Si−O−LaL_2 directly. Although the formation of Si-LaL_2 is also possible, the Si−La stretching band is below our accessible spectral range. Therefore, it is not possible to determine how much of the reaction with the surface is due to partially hydrolyzed precursor, although the intensity of the 928 cm^{-1} band points to almost a full monolayer coverage of Si−O−La bonds. The most intense vibrational mode at 1665 cm^{-1} of the gas phase La precursor does not appear on the surface absorption spectra, confirming that it belongs to the nonreactive gas product (HL) that is easily pumped out during the purge cycle of the ALD process. The broadband around 1300−1600 cm^{-1} originates from the surface amidinate ligand, and methyl groups are also observed in the 2800−3000 cm^{-1} spectral range.

With more ALD cycles, the La_2O_3 phonon modes start to develop in the 450−540 cm^{-1} range (left panel of Figure 3a). There is evidence that these ALD La_2O_3 films are polycrystalline, but it is not possible to determine the structure from the IR spectra. Several broad peaks between 800 and 1200 cm^{-1} are assigned to the Si−O stretching of lanthanum silicate, La−O−Si,[30] because they are located at frequencies lower than typical Si−O vibrations due to a weakening of the Si−O bond from electron density transfer from lanthanum to the Si−O. Spectra taken at near normal incidence (electric field parallel to the interface) indicate that the modes at 985 and 1170 cm^{-1} are polarized perpendicular to the surface; that is, they have characteristics of the longitudinal optical phonons. Altogether, these observations are consistent with the formation of a very thin lanthanum silicate layer in the vicinity of the interface, in addition to the Si−O−La interfacial layer.

As the film gets thicker, carbonate and water (D_2O) are detected in the films, as evidenced by the broad absorption in the 1300−1600 and 2400−2700 cm^{-1} spectral regions, respectively. A doublet centered at 1460, 1415 cm^{-1} and the band at 860 cm^{-1} suggest unidentately bound carbonate species.[31] La_2O_3 can react with ambient CO_2, resulting in carbonate incorporation into the films.[32−36] However, residual CO_2 is negligible inside the reactor, and the film is not exposed to air during the whole ALD process. Therefore, any carbonate present in the film must have been generated by intrinsic surface reactions. It is likely that lanthanum carbonate is produced through thermal decomposition of lanthanum acetate. There is, in fact, evidence of some acetate species present on the surface, characterized by broad bands between about 600 and 700 cm^{-1} and between about 2800 and 3000 cm^{-1} (see Figure 3a). The areas under these bands (and the bands between 1300 and 1600 cm^{-1}) grow almost linearly with the number of ALD cycles. The differential spectra measured after each half-cycle (inset of Figure 3a) show that the intensity of these vibrational modes increases after D_2O pulses rather than after La(^{i}Pr-MeAMD)$_3$ pulses, which suggests that these bands arise from reactions between D_2O and amidinate ligands remaining on the surface. Chemically plausible reactions of this type would include hydrolysis of amidinate ligands first to amides and amines by reaction 1:

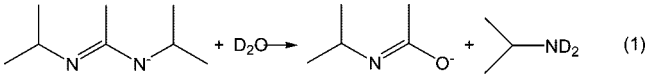

(1)

A second hydrolysis reaction 2 can then convert the amide to acetate and more isopropylamine, which is volatile and should be removed by the vacuum system.

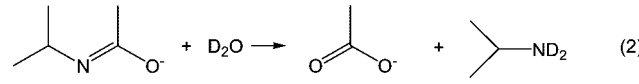

(2)

Some of the resulting acetate ions are likely to remain as impurities because the lanthanum−acetate bond is roughly as strong as a lanthanum−hydroxyl bond. Thus, there is little thermodynamic driving force to hydrolyzing the acetate ions to acetic acid, which would vaporize off the surface. The infrared spectrum of lanthanum acetate includes broad, intense bands at around 1450 and 1550 cm^{-1}, as well as weaker bands between 600 and 700 cm^{-1} and between 2850 and 3000 cm^{-1}.[37] A part of lanthanum acetate is then thermally decomposed on the surface, thus producing lanthanum carbonate that has a doublet centered at 1460, 1415 cm^{-1} and the band at 860 cm^{-1}. Thus, water and acetate ions together can explain all the observed impurity bands.

La atomic density is 5×10^{15} /cm^2, according to ex situ RBS measurements of 20-cycle lanthanum oxide films deposited at 200 °C. Assuming a density of bulk La_2O_3 of 6.51 g/cm^3, the resulting lanthanum oxide film thickness is 21 Å. But due to the presence of lanthanum silicate at the interface and impurities in the film, the overall thickness of the film might be greater. Ex situ spectroscopic ellipsometry measurements on the same sample yield an overall thickness of 23 Å, in close agreement with our estimate.

Post deposition annealing at 500 °C almost completely removes all these broad bands (see Figure 3b) and D_2O (not shown) arising from impurities in the film. Since all these impurities contain oxygen, their thermal decomposition/reaction can provide the excess oxygen necessary to grow the interfacial silicon oxide layer observed upon annealing (see Figure 3b), in agreement with previous observations.[38]

The results in Figure 3b suggest that the incorporation of impurities can be substantially decreased by heating the substrate at moderate temperatures (≤400 °C) without substantially increasing the interfacial SiO_2 layer. Indeed, the intensities in the regions 1300−1600 and 2800−3000 cm^{-1} for acetate/carbonate and 2400−2700 cm^{-1} for D_2O are weakened substantially for ALD growth at 300 °C (Figure 4). The inset of Figure 4 shows the differential spectra around the Si−H stretching mode, each of which is referenced to the previous spectrum. La(^{i}Pr-MeAMD)$_3$ reacts with surface hydrogen very strongly at 300 °C, consuming almost all Si−H bonds in five ALD cycles. Although the amount of interfacial SiO_2 is increased as compared to the same treatment with Si at 200 °C (∼100% increase), the total average thickness of that interfacial layer is estimated to be only ∼5 Å, according to the integrated area under SiO_2 modes, which has been normalized with respect to a chemical oxide grown by wet chemical oxidation of H-terminated Si using the RCA method (∼10 Å). These observations suggest that 300 °C is a good substrate temperature for optimum growth.

There are, however, new features at 1990 and 2110 cm^{-1} observed after each La precursor pulse when Si is held at 300 °C. Their intensities are dramatically reduced after each subsequent D_2O pulse. The frequencies of these two bands are very close to those of Si—H stretching modes on modified Si surfaces, but their integrated areas are much greater than that of the initial Si—H stretching mode. Their origin is likely involving CN, since there is evidence in the literature that the

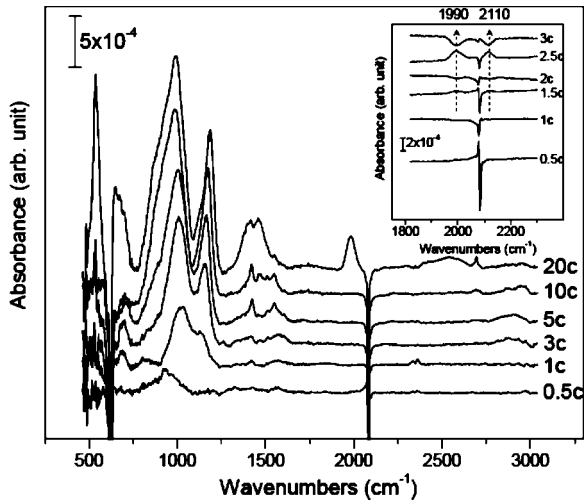

Figure 4. Absorption spectra of H/Si(111) after it is exposed to the first La(^{i}Pr-MeAMD)$_3$ (0.5c), D_2O (1c) and 5th, 10th and 20th cycles of ALD at 300 °C. The inset is the differential spectra of half-cycles from 0.5th to third cycle in the 1900−2200 cm^{-1} range.

stretching vibration of the triple bond (C≡N) in the cyanamide $(N-C\equiv N)^{2-}$ or the double bond (*C*=N) in the carbodiimide $(N=C=N)^{2-}$ occurs around 2000 cm^{-1}, often in the form of two bands.[39] The formation of the cyanamide (or carbodiimide) ions on the surface suggests ligand decomposition at 300 °C through β- or δ-hydrogen transfer within the ligand. Scheme 1 below shows possible decomposition pathways to cyanamide. Initially, β-hydrogen transfers can lead to the formation of NH bonds on the ligand, and propene (C_3H_6) could be produced as a gas phase byproduct. N≡C triple bonds could then be produced through the second β-hydrogen transfer with methane (CH_4) as a byproduct. This N≡C triple bond can also be formed directly by δ-hydrogen transfers from the intact ligand on the surface. Finally, cyanamide could be formed through additional β-hydrogen transfers with propene as a byproduct that is pumped off without further interaction with the surface.

Often, ligand decomposition on the surface leads to further growth within the half-cycle (self-reaction of the precursor), thereby destroying the self-limitation of the reaction. However, in this case, the decomposed ligands are not reactive with further precursor molecules and are removed from the surface by the subsequent water pulse, as evidenced by the loss of the intensity at 1990 and 2110 cm^{-1} (see the differential spectra in the inset of Figure 4). Thus, this ALD reaction remains self-limited, despite the ligand decomposition. In addition, the composition of the film remains the same, whether or not ligand decomposition takes place. In fact, the smaller decomposed ligand facilitates access of more precursor molecules to the surface (smaller steric interactions), speeding up the film growth. The fact that more ligand decomposition is seen at higher surface temperature indicates that there are energy barriers to these decomposition reactions.

Lanthanum oxide is known to be highly hygroscopic, forming lanthanum hydroxide when exposed to water vapor. Lanthanum hydroxide then slowly desorbs water again during lanthanum precursor cycles. CVD reactions can be dominant in these cases, and film thickness derived from ex situ Rutherford backscattering measurements confirms nonuniform film growth. Water adsorption/desorption problems due to the hygroscopic nature of La_2O_3 can be overcome by growing interpenetrating, water-impervious layers, such as Al_2O_3 layers. For instance, Gordon et al.[21] have successfully suppressed CVD reactions by depositing alternating layers of La_2O_3 and Al_2O_3.

To compare the effect of Al−O components in the ALD-grown lanthanum oxide, a full cycle of trimethylaluminum (TMA) and D_2O is introduced after each La(^{i}Pr-MeAMD)$_3$/D_2O cycle. Figure 5a shows differential spectra of H/Si(111) exposed to alternating ALD cycles at 300 °C. Interfacial SiO_2 is formed after the first complete La/D_2O cycle at this temperature in addition to lanthanum silicate, as evidenced by the modes centered around 1034 and 1155

SCHEME 1: Possible Decomposition Pathways from Amidinate Ligand to Cyanamide[a]

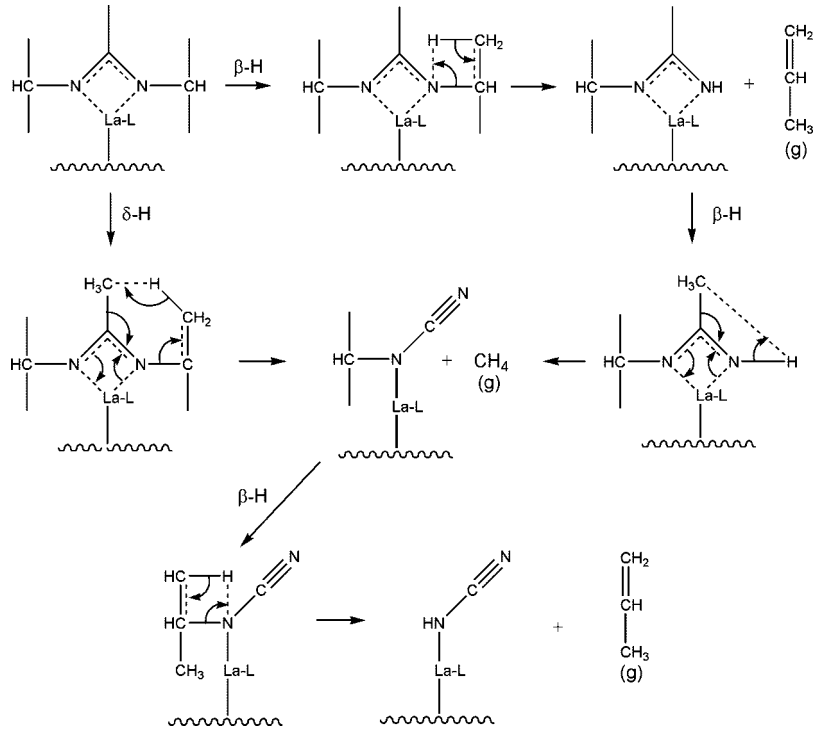

[a] L represents an additional undecomposed amidinate ligand attached to the same La atom.

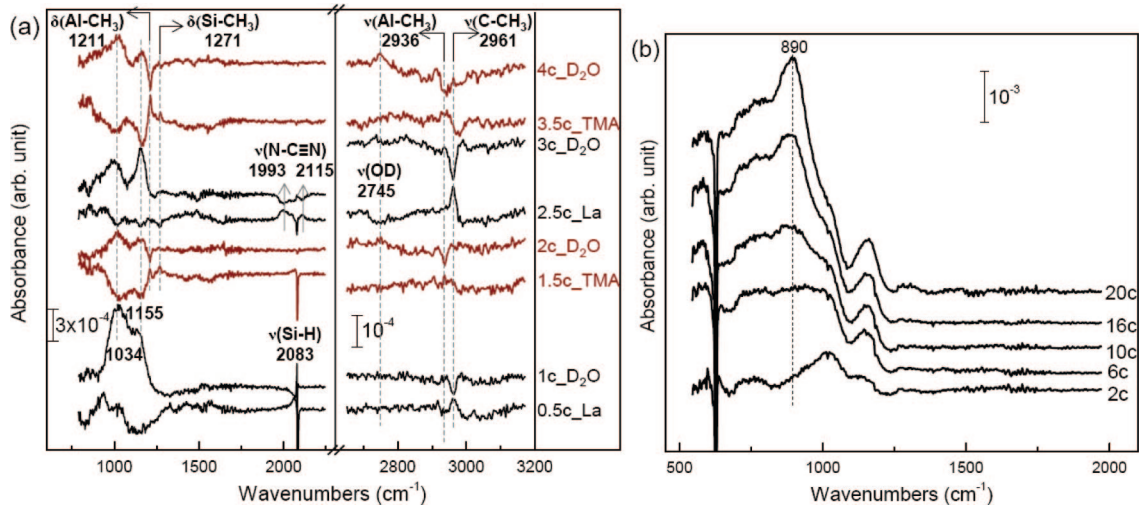

Figure 5. (a) Differential spectra of H/Si(111) upon exposure at 300 °C to La(^{i}Pr-MeAMD)$_3$ (0.5c_La), D_2O (1c_D_2O) and trimethylaluminum (1.5c_TMA), D_2O (2c_D_2O) up to the fourth ALD cycle. Each spectrum is referenced back to the previously treated surface. (b) Absorbance spectra after 2, 6, 10, 16, or 20 cycles, referenced to the initial H/Si(111).

cm^{-1} ("1c_D_2O" in Figure 5a). The slight loss of these modes after the first TMA pulse ("1.5c_TMA" in Figure 5a) shows the disruption of the oxide matrix due to TMA. The vibrational mode at 1211 cm^{-1} is assigned to CH bending of Al-bonded methyl groups. It is lower than that of (Si−O−Al)−CH_3 by ∼6 cm^{-1}, probably because it is in La−O−Al−CH_3 arrangements. This band at 1211 cm^{-1} displays a ligand exchange behavior with the OD band at 2745 cm^{-1} upon D_2O exposure, confirming the expected reaction with Al−CH_3.

The mode at 1271 cm^{-1} has been assigned to the umbrella mode of methyl groups bonded directly to Si atoms,[40] suggesting that there might be some methyl transfer from TMA to the remaining surface H−Si bonds. Interestingly, the second La(^{i}Pr-MeAMD)$_3$ pulse appears to reacts with Si-CH_3, as evidenced by the negative peak at 1271 cm^{-1} (see "2.5c_La"), and the same phenomenon is observed after the third La-precursor dosing (not shown). Surface H atoms are all consumed by then, and the mode at 1271 cm^{-1} does not occur any more after the third La/D_2O cycle. It is not certain why the strong Si−CH_3 bond reacts with La(^{i}Pr-MeAMD)$_3$. On the other hand, TMA pulses after complete La/D_2O cycles appear to react with residual surface amidinate ligands, as evidenced by the loss of the modes around 1300−1600 cm^{-1} ("1.5_TMA" and "3.5c_TMA"). Overall, these interactions between the two metal precursors result in the substantial decrease of C impurity incorporation into the lanthanum aluminate films.

The cyanamide (or carbodiimide) species observed at 1993 and 2115 cm^{-1} due to decomposition of the La precursor react with the subsequent water pulse as illustrated above ("2.5c_La" and "3c_D_2O"). The right panel of Figure 5a shows the frequency of the methyl stretching mode depends on the metal precursor it is attached to. For Al, it is at 2936 cm^{-1}, and for La, it is at 2961 cm^{-1}.

Figure 5b shows the absorbance spectra of the same surface after 20 such alternate ALD cycles referenced to the initial H/Si(111) surface. Compared to the 10-cycle spectrum for pure lanthanum oxide in Figure 5 ("10c"), the vibrational signature of impurities in the 1300−1600 cm^{-1} region is almost completely absent. This suppression of impurity incorporation is mainly due to the interaction of TMA with the surface amidinate ligand, as described above. However, the interfacial SiO_2 growth is comparable because the TMA/D_2O ALD cycle itself produces interfacial oxide at this temperature.[41] A strong peak centered at 890 cm^{-1} appears and can be attributed to La−O−Al phonon absorption. The La atom surface density measured by Rutherford backscattering (3.5×10^{15} cm^2 after 20 cycles at 300 °C) confirms that the lanthanum aluminate film thickness is uniform over the whole sample area, suggesting that CVD reactions are minimized.

IV. Summary and Conclusions

The IR spectroscopic investigation of the growth of La_2O_3 on H-terminated Si surfaces using an amidinate precursor has shown that, due to precursor reaction with residual water vapor, the initial interaction of La(^{i}Pr-MeAMD)$_3$ with H/Si involves the formation of a Si−O−La bond at the interface. Despite the large size of the precursor (i.e., potential steric interactions), there is complete reaction of all surface Si−H bonds within a few ALD cycles (∼10 cycles at 200 °C and 5 cycles at 300 °C). This reaction is facilitated at 300 °C by the fact that the adsorbed precursor readily dissociates to form much smaller cyanamide (or carbodiimide) species that readily react with water pulses. The size and partial reactivity of the precursor contribute to the observation of trapped acetate and carbonate impurities, produced upon water interaction with adsorbed ligands during growth. The concentration of these impurities decreases at higher growth temperatures or upon post annealing, possibly leading to carbon contamination of the films. In general, the growth of pure La_2O_3 films is difficult because they are highly hygroscopic, leading to thickness nonuniformities on a macroscopic scale. Introducing alternating TMA + D_2O ALD cycles suppresses CVD-like reactions and minimizes the acetate/carbonate incorporation.

Acknowledgment. This work was supported by the National Science Foundation (CHE-0415652 and CHE-0354213). The lanthanum precursor was supplied by the Advanced Thin-Film Technologies Group at Rohm and Haas Electronic Materials. We appreciate assistance from Dr. Leonard N. J. Rodriguez and Dr. Harish Bhandari in handling the precursor, and Dr. Leszek Wielunski in taking RBS measurements.

References and Notes

(1) Ritala, M.; Leskelä, M. In *Handbook of Thin Film Materials*; Nalwa, H. S., Ed.; Academic Press, San Diego, 2001; Vol. 1.

(2) Luo, Y.; Yao, Y.; Shen, Q.; Sun, J.; Weng, L. *J. Organomet. Chem.* **2002**, *662*, 144.

(3) Vendemiati, B.; Prini, G.; Meetsma, A.; Hessen, B.; Teuben, J. H.; Traverso, O. *Eur. J. Inorg. Chem.* **2001**, *2001*, 707.
(4) Boere, R. T.; Cole, M. L.; Junk, P. C. *New J. Chem.* **2005**, *29*, 128.
(5) Kissounko, D. A.; Zabalov, M. V.; Brusova, G. P.; Lemenovskii, D. A. *Russ. Chem. Rev.* **2006**, *75*, 351.
(6) Lim, B. S.; Rahtu, A.; Park, J. S.; Gordon, R. G. *Inorg. Chem.* **2003**, *42*, 7951.
(7) Lim, B. S.; Rahtu, A.; Gordon, R. G. *Nat. Mater.* **2003**, *2*, 749.
(8) Dagorne, S.; Guzei, I. A.; Coles, M. P.; Jordan, R. F. *J. Am. Chem. Soc.* **2000**, *122*, 274.
(9) Barker, J.; Kilner, M. *Coord. Chem. Rev.* **1994**, *133*, 219.
(10) Edelmann, F. T. *Chem. Rev.* **1994**, *137*, 403.
(11) Kim, K. H.; Farmer, D. B.; Lehn, J.-S. M.; Rao, P. V.; Gordon, R. G. *Appl. Phys. Lett.* **2006**, *89*, 133512.
(12) Li, Z.; Rahtu, A.; Gordon, R. G. *J. Electrochem. Soc.* **2006**, *153*, C787.
(13) de Rouffignac, P.; Park, J.-S.; Gordon, R. G. *Chem. Mater.* **2005**, *17*, 4808.
(14) de Rouffignac, P.; Yousef, A. P.; Kim, K. H.; Gordon, R. G. *Electrochem. Solid-State Lett.* **2006**, *9*, F45.
(15) de Rouffignac, P.; Gordon, R. G. *Chem. Vapor Dep.* **2006**, *12*, 152.
(16) Li, H.; Farmer, D. B.; Gordon, R. G.; Lin, Y.; Vlassak, J. *J. Electrochem. Soc.* **2007**, *154*, D642.
(17) Devine, R. A. B. *J. Appl. Phys.* **2003**, *93*, 9938.
(18) Yamada, H.; Shmizu, T.; Kurokawa, A.; Ishii, K.; Suzuki, E. *J. Electrochem. Soc.* **2003**, *150*, G429.
(19) Jin, H. J.; Choi, D. J.; Kim, K. H.; Oh, K. Y.; Hwang, C. J. *Jpn. J. Appl. Phys., Part 1* **2003**, *42*, 3519.
(20) Wu, Y. H.; Yang, M. Y.; Chin, A.; Chen, W. J.; Kwei, C. M. *IEEE Electron Device Lett.* **2000**, *21*, 341.
(21) Lim, B. S.; Rahtu, A.; Rouffignac, P. D.; Gordon, R. G. *Appl. Phys. Lett.* **2004**, *84*, 3957.
(22) Gordon, R. G.; Lehn, J.-S.; Liu, Y.; Kim, K. H.; Li, Z.; Coulter, M.; Li, H.; Pugh, R.; Shenai, D. AVS 75th International Conference on Atomic Layer Deposition, San Jose, CA, 2007 (published on CD-ROM by AVS).
(23) Reinhardt, K. A.; Kern, W. *Handbook of Silicon Wafer Cleaning Technology*, 2nd ed.; Andrew, W., Ed.; Norwich: New York, 2007.
(24) Chabal, Y. J. *Surf. Sci. Rep.* **1988**, *8*, 211.
(25) Perdew, J. P.; Burke, K.; Ernzerhof, M. *Phys. Rev. Lett.* **1996**, *77*, 3865.
(26) Delley, B. *J. Chem. Phys.* **2000**, *113* (18), 7756.
(27) Delley, B. *Phys. Rev. B* **2002**, *66*, 155125.
(28) Wilkins, J. D. *J. Organomet. Chem.* **1974**, *80*, 349.
(29) Ono, H.; Katsumata, T. *Appl. Phys. Lett.* **2001**, *78*, 1832.
(30) Yamamoto, T.; Izumi, Y.; Hashimoto, H.; Oosawa, M.; Sugita, Y. *Jap. J. Appl. Phys.* **2006**, *45*, 6196.
(31) Klingenberg, B.; Vannice, M. A. *Chem. Mater.* **1996**, *8*, 2755.
(32) Suzuki, M.; Kagawa, M.; Syono, Y.; Hirai, T. *J. Cryst. Growth* **1991**, *112*, 621.
(33) De Asah, A. M.; Critchley, J. T. S.; Nix, R. M. *Surf. Sci.* **1998**, *405*, 201.
(34) Gougousi, T.; Niu, D.; Ashcraft, R. W.; Parsons, G. N. *Appl. Phys. Lett.* **2003**, *83*, 3543.
(35) Nieminen, M.; Putkonen, M.; Niinisto, L. *Appl. Surf. Sci.* **2001**, *174*, 155.
(36) Cheng, J. B.; Li, A. D.; Shao, Q. Y.; Ling, H. Q.; Wu, D.; Yang, Y.; Bao, Y. J.; Wang, M.; Liu, Z. G.; Ming, N. B. *Appl. Surf. Sci.* **2004**, *233*, 91.
(37) da Rocha, S. M. R.; da Silva, C. A.; Abrao, A. *J. Alloys Compd.* **2002**, *344*, 389.
(38) Leskelä, M.; Ninistö, L. In *Handbook on the Physics and Chemistry of Rare Earths*; Gschneider, K. A., Jr., Eyring, L., Eds.; Elsevier: Amsterdam, 1986; Vol. 8, chapter 56.
(39) Reckeweg, O.; Simon, A. *Z. Naturforsch.* **2003**, *58b*, 1097.
(40) Kwon, J.; Dai, M.; Halls, M. D.; Chabal, Y. J. *Chem. Mater.* **2008**, *20*, 3248.
(41) Frank, M. M.; Chabal, Y. J.; Wilk, G. D. *Apply. Phys. Lett.* **2003**, *82*, 4758.

JP806027M